

Original Article

PRELIMINARY STUDIES ON BRAIN TARGETING OF INTRANASAL ATOMOXETINE LIPOSOMES

AMRUTA V. VAIDYA<sup>1</sup>, UJWALA A. SHINDE<sup>2\*</sup>, HEMANT H. SHIMPI<sup>3</sup>

<sup>1,2</sup>Department of Pharmaceutics, Bombay College of Pharmacy, Kalina, Santacruz (E), Mumbai, India, <sup>3</sup>Radiation Medicine Centre, Tata Memorial Hospital, Parel, Mumbai, India  
Email: [ujwalashinde29@gmail.com](mailto:ujwalashinde29@gmail.com)

Received: 20 Sep 2015 Revised and Accepted: 03 Feb 2016

ABSTRACT

**Objective:** The objective of the present study was to evaluate the enhancement in brain uptake of liposomes containing atomoxetine (ATX-Lipo) for intranasal delivery in the management of Attention Deficit Hyperactivity Disorder (ADHD).

**Methods:** ATX-Lipo and ATX mucoadhesive liposomes (ATX-Muco Lipo) with and without a vasoconstrictor phenylephrine (PHE) were prepared by lipid film hydration method and characterized for physicochemical parameters. Biodistribution and pharmacokinetic evaluation of ATX-Lipo in the brain and blood of Sprague Dawley rats following intranasal (i. n.) and intravenous (i. v.) administrations were examined using optimized technetium-labeled (<sup>99m</sup>Tc-labeled) atomoxetine formulations. Gamma scintigraphy imaging was performed in Sprague Dawley rats.

**Results:** ATX-Lipo and ATX-Muco Lipo were found to be stable with average particle size of 404.35±1.86 nm and 510.50±1.22 nm respectively. <sup>99m</sup>Tc tagged ATX-Lipo, ATX-Muco Lipo, ATX+PHE-Muco Lipo and ATX solution were found to be stable and suitable for *in vivo* studies. On comparing ATX concentrations after i. n. administrations of ATX-Lipo, ATX-Muco Lipo and ATX+PHE-Muco Lipo and i. v. administration of ATX-Lipo, brain/blood uptake ratios (BBR) at 30 min were found to be 0.161, 1.255, 0.331, and 0.003 respectively. These results revealed effective brain targeting following i. n. administration of mucoadhesive ATX liposomes. Higher drug targeting efficiency (% DTE) and direct transport percentage (%DTP) for mucoadhesive liposomes indicated considerable brain targeting from ATX-Muco liposomes. Gamma scintigraphy imaging of the rat brain conclusively demonstrated the greater extent of transport of atomoxetine by ATX+PHE-Muco Lipo (i. n.), when compared with ATX solution (i. n.) into the rat brain.

**Conclusion:** This preliminary investigation demonstrates a considerable extent of transport of ATX into the brain through i. n. ATX+PHE-Muco Lipo, which may prove to be a new platform for better management of ADHD.

**Keywords:** Intranasal delivery, Brain targeting, Mucoadhesive liposomes, Vasoconstrictor, Radiolabeling, Drug targeting efficiency, Direct transport percentage, Gamma scintigraphy.

© 2016 The Authors. Published by Innovare Academic Sciences Pvt Ltd. This is an open access article under the CC-BY license (<http://creativecommons.org/licenses/by/4.0/>)

INTRODUCTION

Attention Deficit Hyperactivity disorder (ADHD) or hyperkinetic disorder is one of the most common neurodevelopmental disorders affecting approximately 5% of children and adolescents worldwide. In approximately 80% of children with ADHD, symptoms may persist even in adolescence and continue up to adulthood [1]. Children and youths who suffer from ADHD are most likely troubled with hyperactivity, impulsivity, distractibility and inattention. Older adults most likely suffer from attention difficulties and perhaps executive function deficits. ADHD has gained worldwide prevalence and the treatment of this neurodevelopmental disorder requires all-day symptom control and to improve patient compliance especially in children by providing flexibility in the onset and duration of action of any specific medication regardless of the child's variable daily activities or needs [2]. Pharmacological and behavioural interventions have been explored for the treatment of ADHD. Pharmacotherapy mainly with psychostimulants like methylphenidate and antidepressants remains the standard practice for ADHD management [3]. However, stimulants suffer from drawbacks of reduced appetite, delayed onset of sleep and also the risk of misuse and abuse, thus reducing patient compliance.

Atomoxetine (ATX) a non-stimulant has come to the forefront for the treatment of ADHD due to its high water solubility, favourable dissolution and intestinal permeability characteristics (BCS Class I) because of which it shows rapid absorption on oral administration. ATX is the first non-stimulant approved by the US-FDA and is an effective alternative to stimulants, especially for patients who have comorbidities that contraindicate their use. However, metabolism of ATX is governed by the genetic polymorphism of the enzyme CYP2D6. This enzyme can lead to higher first-pass metabolism in the case of extensive metabolizer of this drug and thus reduce the absolute oral bioavailability of ATX [4].

The management of ADHD involves use of immediate release, extended release, and osmotic release oral dosage forms in addition to transdermal patch; however, the onset of action is longer for a drug delivered by the oral route. Also, because of constraints of blood-brain barrier time required to achieve effective concentration at site of action i.e. the brain is greater. Expression of efflux transporters in tissue compartments like the gastrointestinal tract and brain capillary endothelial cells limits the oral absorption and central nervous system entry (CNS) of many drugs [5]. Hence, alternative routes of administration are explored. The intranasal administration appears to be one such non-invasive and convenient route to target therapeutic moieties rapidly to the CNS [6, 8]. To state a few, the nasal route offers advantages of fast absorption of drug, circumventing first-pass metabolism and enhanced bioavailability at lower doses [9, 10]. Even in case of the intranasal route, the diffusion of drugs from the blood into the brain depends mainly upon the ability of the biologically active molecule to cross lipid membranes. Furthermore, in case of hydrophilic drugs, to achieve therapeutic concentrations by overcoming the blood-brain barrier is a challenging task.

Hence, various strategies are in progress to deliver drugs intranasally into the brain which includes lipophilic analogues, prodrugs, microspheres, nano particles, liposomes, etc. [11]. Such targeted nose-to-brain drug delivery systems increase the therapeutic efficacy of CNS-acting drugs thereby reducing any systemic side effects as well.

Liposomes have the advantages of being biodegradable, easy to scale up, greater specificity towards cells or tissue, protect drug degradation from nasal enzymes and thus make it a suitable colloidal carrier for intranasal delivery of the drug by allowing better access across the BBB compared to other carriers [12, 13]. However, the limitations posed by intranasal route can be slow diffusion of most drugs, and a

limited volume accommodated by the nasal cavity (150 µl/nostril) due to which the excess formulation will drain into the pharynx and be swallowed [14]. The addition of mucoadhesive agent is reported to enhance retention of formulation in the nasal cavity.

Dhuria *et al.* and many others have demonstrated that inclusion of a short-acting vasoconstrictor in nasal formulations to enhance intranasal drug targeting to multiple brain area while significantly reducing systemic absorption [15]. This may hold relevance for the treatment of various neurological disorders. Highlighting the above aspects, the work undertaken relates to biopharmaceutical evaluation of ATX-Lipo for brain targeting when administered intranasally. Furthermore, the objective of the study was to evaluate brain uptake efficiency in the presence of vasoconstrictor (phenylephrine) in ATX liposomes.

## MATERIALS AND METHODS

### Materials and reagents

ATX pure powder was obtained as a gift sample from Panchsheel Organics Ltd. (Mumbai, India). Phospholipon 90G was a gift sample from Lipoid, Germany and HPMC K4M as a gift sample from Colorcon, Mumbai. Chloroform AR, Disodium hydrogen orthophosphate AR, Potassium dihydrogen orthophosphate AR, Sodium chloride AR were purchased from S. D. Fine Chem. Ltd, India. Filtered distilled water was used throughout the study. All other chemicals and solvents were of analytical reagent grade and used as received without any further purification.

### Animals

Animal experiments were carried out in accordance with the guidelines of the institutional ethics committee (Radiation Medicine Centre, Bhabha Atomic Research Centre, and Mumbai). Female Sprague Dawley rats are having a body weight in the range of 250–300 g were used for the study. The animals were housed at a temperature of 22±3 °C and 65% relative humidity. Throughout the experiments, the animals were fed with a standard rat diet and were provided with clean drinking water *ad libitum*.

### Methods

#### Preparation and characterization of ATX liposomes

The liposomes of ATX were prepared by adapting the procedure described by Rania, M *et. al* for the lipid film hydration method [16]. Briefly a mixture of phospholipid, Phospholipon 90G and cholesterol in a molar ratio of 4:1 were dissolved in chloroform in a 100 ml round bottom flask. The solvent mixture was then evaporated in rotavapor apparatus (Superfit, India) at 40 °C (pressure 400-600 mmHg) until a dry film was formed on the inner circumference of the round bottom flask. The dry film thus formed was hydrated with phosphate buffer saline (PBS) (pH= 7.4) containing drug (5 mg/ml) at 60 °C. The dispersion was hand shaken and vortex mixed on cyclomixer (Remi, Mumbai) to get a homogenous mixture of ATX-Lipo. The mucoadhesive liposomes of ATX were formulated by adding required volume of the polymer solution of HPMC K4M (0.5% w/v) to the final volume of hydration medium to get ATX-Muco Lipo. To this liposomal suspension of ATX-Muco Lipo required a volume of 0.05% PHE solution was added to get ATX+PHE-Muco Lipo. The particle size distribution of the liposomes was evaluated by Dynamic light scattering spectroscopy (DLS) using Zetasizer Nano ZS (Malvern, U. K.). ATX-Lipo samples were further diluted with 0.45µ filtered distilled water to ensure that light scattering intensity was within instrument's sensitivity range. These samples were placed in transparent polystyrene cuvettes (1 cm<sup>2</sup>) and loaded in thermo stated chamber. Light scattering was monitored at an angle of 173 ° to the incident beam, and all measurements were made in duplicates at 25 °C.

The zeta potential of liposomal samples was measured by Laser Doppler velocimetry using Zetasizer Nano ZS at 25 °C (Malvern, U. K.). The zeta potential of a liposome preparation can help to predict the fate of the liposomes *in vivo*. Samples diluted 1 in 10 with filtered distilled water were placed in a disposable capillary cell and loaded in the thermo stated chamber. The scattered light detected from samples while a zeta potential measurement is made at the forward angle of 12 ° and all measurements were made in duplicates at 25 °C.

The entrapment efficiency of ATX in liposomes was determined indirectly.

Briefly, the formulated ATX liposomes were separated from un-entrapped ATX by ultra-centrifugation at 80,000 rpm for 60 min at 4 °C using Optima Max XP ultracentrifuge (Beckman Coulter, USA). The collected supernatant after suitable dilution with PBS pH 7.4 was quantified by validated UV spectroscopy method at 270 nm. The ATX entrapment efficiency (EE) of liposomes was calculated as indicated below:

%Entrapment efficiency

$$= \frac{\text{Total amount of ATX loaded} - \text{Free ATX in supernatant}}{\text{Total amount of ATX loaded}} \times 100$$

Mucoadhesion potential was determined by modified pan balance fabricated in the laboratory [17]. The mucoadhesive force was calculated using the equation,  $F = W \cdot g / a$  where, F= Mucoadhesion force (dynes/cm<sup>2</sup>), W= minimum weight in grams required to break the mucoadhesive bond, g= acceleration due to gravity (cm/s<sup>2</sup>) and a= surface area of the slide onto which the formulation was applied.

### Pharmacokinetic study

The protocol for animal experimentation was approved by BARC Animal Ethics Committee (Protocol no: BAEC/13/15). The study was done in collaboration with Radiation Medicine Centre, Tata Memorial Hospital, Parel, and Mumbai.

#### Preparation of technetium-tagged formulations

ATX-Lipo, ATX-Muco Lipo, ATX+PHE-Muco Lipo and ATX solution preparations were tagged with radionuclide <sup>99m</sup>Tc by the direct labeling method [18]. To 1.0 ml of ATX liposomal formulations (5 mg/ml) at pH=6, 100 µl of stannous chloride (1 mg/ml in 0.01N HCl) was added. Likewise, 1.0 ml of ATX solution prepared in saline was mixed with 50 µl of above stannous chloride solution. These sample mixtures of ATX liposomal formulations and ATX drug solution were shaken well and incubated for 10 min at room temperature, followed by addition of 1 ml of sterile <sup>99m</sup>Tc-pertechnetate (75-400 MBq) and the resultant reaction mixtures were again incubated for 20 min at room temperature.

The radiochemical purity of <sup>99m</sup>Tc tagged ATX formulations was determined by ascending instant TLC using silica gel coated aluminium backed sheets and acetone as the mobile phase. The <sup>99m</sup>Tc tagged formulation complex and the <sup>99m</sup>Tc tagged drug complex remain at the point of the spots while free technetium moves towards the solvent front.

The radiolabeling efficiency was calculated using equation given below:

$$\% \text{ Labeling efficiency} = \frac{\text{Total counts} - \text{Counts of free Technetium}}{\text{Total counts}} \times 100$$

The effects of incubation time and stannous chloride concentration on radiolabeling efficiency were evaluated to achieve optimum conditions.

The stability of the <sup>99m</sup>Tc tagged ATX formulations and drug complexes were also assessed at 37±2 °C up to 3 h. The optimized, stable <sup>99m</sup>Tc tagged formulations of ATX were used for bio distribution study in rats.

### Bio-distribution studies

Female Sprague Dawley rats weighing between 200-250g were selected for the study. The <sup>99m</sup>Tc tagged complexes of <sup>99m</sup>Tc-ATX-Lipo, <sup>99m</sup>Tc-ATX-Muco Lipo, and <sup>99m</sup>Tc-ATX+PHE Muco Lipo were administered intranasally. Similarly <sup>99m</sup>Tc-ATX-Lipo and <sup>99m</sup>Tc-ATX solution were injected through leg vein of Sprague Dawley rats. The administration and dosing details of the study protocol have been stated in table 1. Prior to nasal and intravenous administration of the formulations, the rats were anaesthetized using 50 mg/kg ketamine intramuscular injection. The formulations were instilled

into the nostrils with the help of micropipette (10-100µl) attached to a low-density polyethylene tube having 0.1 mm internal diameter at the delivery site. The rats were placed in supine position with a head angle of 90° while dosing and even after dosing for 1 min in order to prevent drainage of the dose. Rats were sacrificed at predetermined time intervals, and blood was collected using cardiac puncture. Subsequently, different organs including brain were isolated and <sup>99m</sup>Tc radioactivity associated with each of them was counted using well-type gamma counter and percent uptake was calculated using

following equation:

%Radioactivity

$$= \frac{\text{Radioactivity counts in an organ} - \text{Background count of instrument}}{\text{Total radioactivity counts in the body of rat}} \times 100$$

Unit of measurement: counts per second (cps)

**Table 1: Study details of bio distribution study**

Formulation	Administration	Volume	Dose	Euthanasia time points* (min)
<sup>99m</sup> Tc ATX Liposomes	Intranasal	50 µl per nostril	125 µci/100 µl+0.125 mg atomoxetine	10, 30, 60, 180
<sup>99m</sup> Tc ATX Liposomes	Intravenous	100 µl	125 µci/100 µl+0.125 mg atomoxetine	10, 30, 60, 180

\* n=3/time point

To evaluate the brain-targeting efficiency, two indexes drug targeting efficiency (DTE %) and nose-to-brain direct transport percentage (DTP %) of ATX were determined. DTE (%) represents time average partitioning ratio, as derived from Equation (1). Direct transport percentage which defines nose-brain direct transport (DTP, %) was also calculated which is shown in equation (2).

$$\text{DTE\%} = \frac{(\text{AUC brain/AUC blood})_{i.n.}}{(\text{AUC brain/AUC blood})_{i.v.}} \times 100 \quad (1)$$

$$\text{DTP \%} = (\text{B}_{i.n.} - \text{B}_x / \text{B}_{i.n.}) \times 100 \quad (2)$$

Where,  $B_x = (B_{i.v.} / P_{i.v.}) \times P_{i.n.} \times B_x$

$B_x$  is the AUC brain fraction contributed by systemic circulation through the BBB following intranasal administration,  $B_{i.v.}$  is the  $AUC_{0-180}$  (brain) following intravenous administration,  $P_{i.v.}$  is the  $AUC_{0-180}$  (blood) following intravenous administration,  $B_{i.n.}$  is the  $AUC_{0-180}$  (brain) following intranasal administration,  $P_{i.n.}$  is the  $AUC_{0-180}$  (blood) following intranasal administration, AUC: Area under the curve. DTP (%) and DTE (%) were calculated using tissue/organ distribution data following intranasal and intravenous administrations [19].

### Gamma scintigraphy imaging

Sprague Dawley rats were selected for the study. The <sup>99m</sup>Tc tagged complexes of <sup>99m</sup>Tc-ATX-Sol and <sup>99m</sup>Tc-ATX+PHE Muco Lipo were administered i. n. (50 µl in each nostril) at a dose of 2 mg/kg body weight and kept for 30 min. The rats were held back in slanted position during nasal administration of the formulations. The rats were then anaesthetized using an intraperitoneal injection of ketamine

and xylazine (20 mg/kg body weight) 10 min before imaging. The rat was fixed on a board in posterior-anterior position, and imaging was performed using e-Cam Dual Sign, Siemens gamma camera.

### Statistical analysis

All data are reported as mean±SD and the difference between the groups was tested using Student's t-test at the level of P<0.05. Pharmacokinetic parameters like AUC were calculated using Microsoft Excel software.

## RESULTS AND DISCUSSION

### Formulation development and characterization

Liposomes can be prepared by a number of methods which includes ether injection method, handshaking method (Lipid film hydration technique), reverse phase evaporation technique, transmembrane pH gradient method. For the preparation of ATX loaded liposomes only lipid film hydration and ether injection were attempted, the results of which are depicted in table 2.

The formed liposomal dispersion was homogeneous, and opaque, white in colour and all were stable for 24 h. It was also observed that the liposomes prepared with saturated lipid (PL 90H) and cholesterol in molar ratio 2:1 showed larger particle size compared to unsaturated lipids (PL 90G, S-100 and EPC). The entrapment efficiency was found to be low. It could be due to saturated nature of lipid, i.e. PL 90H having lipophilic nature which could possibly be competing with hydrophilic ATX in the lipid bilayer and reducing the entrapment of ATX. Glavas-Dodov *et al.* have reported similar observations for 5-flourouracil [20].

**Table 2: Entrapment efficiency, particle size, polydispersity index (PI) and zeta potential of ATX loaded liposomes (n=3)**

S. No.	PC: MA	Lipid content	Method	Molar ratio	Percent entrapment	Particle size	Polydispersity index (PDI)	Zeta potential
1	PL 90H: CH	50 mg	LFH	2:1	10.29±1.64	7854.00	1.00	7.39
2	S-100:CH	50 mg	LFH	1:1	39.13±3.50	315.10	0.43	28.40
3	S-100:CH	50 mg	LFH	2:1	54.89±4.72	445.75	0.52	35.00
4	S-100:CH	50 mg	Ether	2:1	36.25±4.63	661.20	0.64	14.70
5	S-100:CH	50 mg	LFH	3:1	61.00±2.83	394.30	0.8	40.90
6	EPC: CH	50 mg	LFH	1:1	45.50±3.96	591.85	0.58	23.00
7	EPC: CH	50 mg	LFH	2:1	46.26±4.23	351.00	0.58	22.30
8	EPC: CH	50 mg	LFH	3:1	51.16±4.37	345.65	0.55	28.10
9	PL 90G: CH	50 mg	LFH	1:1	46.25±0.71	413.45	0.40	24.00
10	PL 90G: CH	50 mg	LFH	2:1	53.57±1.27	484.60	0.30	34.15
11	PL 90G: CH	50 mg	Ether	2:1	37.00±3.68	322.60	0.65	15.10
12	PL 90G: CH	50 mg	LFH	3:1	62.00±3.22	531.65	0.28	36.70
13	PL 90G: CH	50 mg	LFH	2:3	27.80±0.85	884.05	0.61	25.55
14	PL 90G: CH	75 mg	LFH	4:1	78.31±1.85	404.35	0.41	40.65

PC: Phosphatidylcholine, MA: Membrane additive, LFH: Lipid Film Hydration method, Ether: Ether injection method, PL 90H: Hydrogenated Phospholipon 90H, PL 90G: Phospholipon 90G, EPC: Egg phosphatidylcholine, CH = Cholesterol.

It was also observed that all liposomes prepared with unsaturated phospholipids allowed better entrapment of drug in the bilayer due to the kinks formed by cis-trans conformational changes of unsaturated lipids. As the molar ratio of phospholipids, drug entrapment increased with increase in particle size and PDI of liposomes. Liposomes prepared by adapting ether injection method resulted in only 37.00±3.68% entrapment of ATX as

compared to liposomes prepared by lipid film hydration i.e. 53.57±1.27%.

Liposomes fabricated from either injection are mostly large unilamellar vesicles (LUV). Large unilamellar vesicles contain less bilayer compared to multilamellar vesicles and hence affect the entrapment efficiency of ATX loaded liposomes [21].

**Table 3: Characterization parameters of optimized ATX liposomes\***

Formulation	Particle size (nm)	Zeta potential (mV)	Percent entrapment efficiency
ATX-Lipo	404.35±1.86	+40.65±0.89	78.31±1.85
ATX-Muco Lipo	510.50±1.22	+37.80±1.98	76.54±2.14

\*Parameters are derived using mean±SD, n=3

The particle size range of 404.35±1.86 nm and 510.50±1.22 nm and PDI of 0.310±0.06 and 0.257±0.01 for ATX-Lipo and ATX-Muco Lipo respectively indicated that the liposomes approached a mono-dispersed stable drug delivery system. The zeta potential of ATX-Lipo and ATX-Muco Lipo was found to be +40.65±0.89 mV and +37.80±1.98 mV respectively. The acquired values of higher positive charge could be attributed to surface deposition of the drug which is cationically charged at pH value below 9 (since pKa is 10.13) resulting in greater colloidal stability due to higher repulsion between particles [22, 23]. The optimized ratio of Phospholipon 90G and cholesterol (4:1) used for the formulation of liposomes gave good entrapment efficiencies of 78.31±1.85 % and 76.54±2.14 % for ATX-Lipo and ATX-Muco Lipo respectively.

From the results of the preliminary screening, as shown in table 2, the suitable phospholipid and membrane additive for encapsulation of ATX was Phospholipon 90G and Cholesterol respectively. Lipid film hydration technique described by Rania M *et al.* was adapted for encapsulation of ATX in liposomes. As it has been reported that varying the molar ratio of phospholipid: cholesterol affects particle size, drug entrapment efficiency and zeta potential, hence in the present study too ATX liposomes were optimized by changing these variables.

ATX liposomal formulations were thus prepared using lipids Phospholipon-90G and cholesterol in a fixed ratio of 4:1. HPMC K4M (0.5% w/w) was used as the mucoadhesive polymer, and Phenylephrine (PHE) (0.05% w/v) was added as a vasoconstrictor in ATX liposomal formulations to obtain ATX-Muco Lipo and ATX+PHE-Muco Lipo respectively. The formulated ATX-Lipo and ATX-Muco Lipo were then characterized for physicochemical parameters as depicted in table 3.

#### Pharmacokinetic evaluation

ATX-Lipo, ATX-Muco Lipo and ATX+PHE-Muco Lipo were effectively tagged with <sup>99m</sup>Tc and optimized for maximum radiolabeling efficiency and stability. Radiochemical purity achieved was 96.22% for ATX-Lipo at the end of 180 min (180 min

was chosen for stability study of the radiolabeled formulations since it was the last time point for the sacrifice of rats). The optimal SnCl<sub>2</sub> concentration was found to be 100 µl (1 mg/ml) for ATX liposomal formulations with an incubation time of 20 min. Thus, the radiolabeled formulations were found suitable for the pharmacokinetic study of ATX in rats.

Bio distribution studies of <sup>99m</sup>Tc formulations following i. n. administration (ATX-Lipo, ATX-Muco Lipo and ATX+PHE-Muco Lipo) and i. v. administration (ATX-Lipo) on Sprague-Dawley rats were performed, and the radioactivity was estimated at different time intervals up to 180 min which is shown in table 4.

The brain/blood ratios of the drug at all sampling time points for different formulations are graphically represented in fig. 1. The pharmacokinetic parameters were calculated from fig. 2 and 3 and were recorded in table 5.

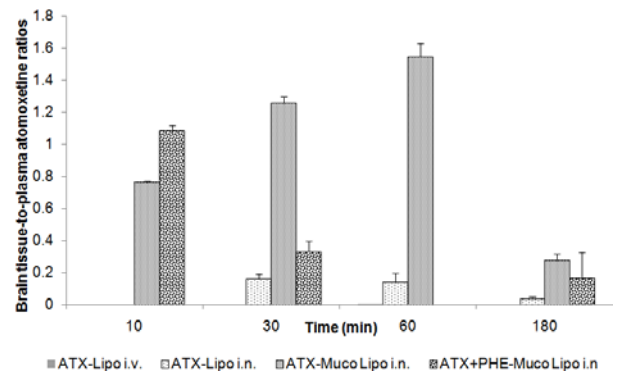


**Fig. 1: Brain tissue-to-plasma atomoxetine concentration ratios as a function of time following intranasal and intravenous liposomes administration respectively in rats. The values represent mean±SD of three animals**

**Table 4: Compartmental distribution <sup>99m</sup>Tc-ATX solution (intravenous), <sup>99m</sup>Tc-ATX Lipo (intranasal), <sup>99m</sup>Tc-ATX Muco Lipo (intranasal), <sup>99m</sup>Tc-ATX+PHE Lipo (intranasal), <sup>99m</sup>Tc-ATX+PHE Muco Lipo (intranasal and <sup>99m</sup>Tc-ATX Lipo (intravenous) at different time intervals in normal Sprague Dawley rats (n=3)\***

Formulation and route of administration	Organ	10 min	30 min	60 min	180 min
ATX Lipo i.v.	Blood	19.76±0.074	10.26±0.085	6.4±0.040	3.38±0.036
	Brain	0.0965±0.24	0.0317±0.012	0.066±0.063	0.0131±0.14
ATX Lipo i.n.	Blood	0.408±0.094	0.154±0.032	0.123±0.18	0.281±0.082
	Brain	0	0.0248±0.056	0.017±0.04	0.01±0.09
ATX Muco Lipo i.n.	Blood	0.169±0.010	0.09±0.09	0.141±0.02	0.141±0.03
	Brain	0.065±0.35	0.0565±0.057	0.109±0.049	0.039±0.42
ATX+PHE Muco Lipo i.n.	Blood	0.023±0.006	0.455±0.033	0.013±0.058	0.291±0.011
	Brain	0.025±0.014	0.151±0.091	0	0.048±0.042

\*The rats were administered with approximately 5 mCi <sup>99m</sup>Tc-atomoxetine and the radioactivity was measured in percentage per gram of tissue of the administered dose. Each value is the mean±SD.

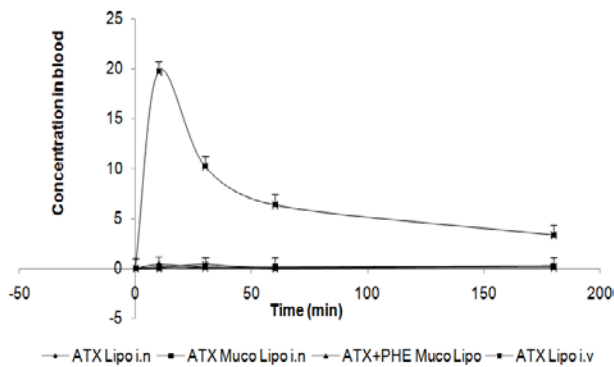


**Fig. 2: Blood concentrations vs. time (min) plot following intranasal and intravenous administrations of  $^{99m}\text{Tc}$ -atomoxetine formulations. The values represent mean $\pm$ SD of three animals,  $p < 0.05$**

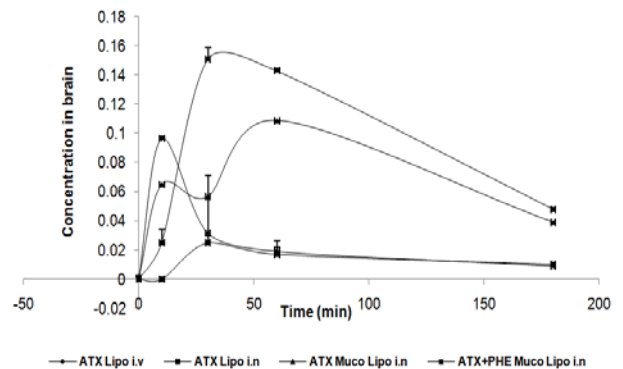


**Fig. 3: Brain concentrations vs. time (min) plot following intranasal and intravenous administrations of  $^{99m}\text{Tc}$ -atomoxetine formulations. The values represent mean $\pm$ SD of three animals,  $p < 0.05$**

**Table 5: Pharmacokinetic parameters of  $^{99m}\text{Tc}$  labelled ATX formulations and ATX solution\***

Formulation	Organ/Tissue	C max (%)	t max (min)	AUC <sub>0-180 min</sub> (min %/g)
ATX-Lipo i.v.	Blood	19.76 $\pm$ 0.24	10	300.2 $\pm$ 0.45
	Brain	0.0965 $\pm$ 0.247	10	1.282 $\pm$ 0.04
ATX-Lipo i.n.	Blood	0.408 $\pm$ 0.094	10	5.62 $\pm$ 0.16
	Brain	0.0248 $\pm$ 0.566	30	0.627 $\pm$ 0.02
ATX-Muco Lipo i.n.	Blood	0.169 $\pm$ 0.01	10	2.59 $\pm$ 0.15
	Brain	0.109 $\pm$ 0.049	60	8.88 $\pm$ 0.08
ATX+PHE Muco Lipo i.n.	Blood	0.455 $\pm$ 0.033	30	7.02 $\pm$ 0.05
	Brain	0.151 $\pm$ 0.091	30	2.26 $\pm$ 0.07

The rats were administered with approximately 5 mCi  $^{99m}\text{Tc}$ -atomoxetine and the radioactivity was m, \* Parameters are derived using mean $\pm$ SD, n=3

The pharmacokinetic studies revealed that the maximum concentrations ( $C_{\text{max}}$ ) of the drug in the brain and blood after i. n. and i. v. administration in rats were attained at different  $t_{\text{max}}$  values. Considering the concentration of drug achieved in the brain at a particular time interval, in the case of intranasal ATX-Lipo a lower  $C_{\text{max}}$  value (0.0248) was attained at a  $t_{\text{max}}$  of 30 min whereas the  $C_{\text{max}}$  (0.109) for intranasal ATX-Muco Lipo was achieved at  $t_{\text{max}}$  of 60 min.

The lower  $C_{\text{max}}$  in brain for intranasal ATX-Lipo may be because of reduced residence time of the formulation due to nasolacrimal drainage. The observed higher  $C_{\text{max}}$  value for intranasal ATX-Muco Lipo (0.109) at 60 min could be attributed to the viscous nature and crosslinking properties of the mucoadhesive polymer incorporated in the liposomal formulation. A similar observation has been reported by Ugwoke, M. *et al.* for nasal mucoadhesive delivery of Apomorphine [24] as a powder dosage form.

The highest  $C_{\text{max}}$  value in the brain (0.151) was achieved at 30 min when ATX+PHE-Muco Lipo was administered intranasally. PHE a vasoconstrictor is clinically known to be given in conjunction with local anaesthetics to prevent wash away of local anaesthetic from the site of action thus prolonging its effect at that site. The similar effect would be attributed when ATX+PHE-Muco Lipo was administered. Dhuria *et al.* have also demonstrated the higher brain uptake of intranasal therapeutic neuropeptides when phenylephrine was incorporated as a vasoconstrictor in their formulation [15].

The increased concentration or activity in blood seen for ATX+PHE-Muco Lipo even in the presence of vasoconstrictor phenylephrine is unusual as seen in table 5. In a study done by Charlton *et al.* when ephedrine was co-administered as a vasoconstrictor along with the drug containing nasal formulation, higher drug blood concentrations were observed [25]. However, in other similar studies [26, 27] it was reported that vasoconstrictors were applied before initiating drug administration instead of co-administering with the nasal formulation. This indicated that in the present study application of the vasoconstrictor PHE prior to intranasal administration of ATX

liposomal formulation instead of co-administration might have increased the probability of greater transport to the brain.

From, table 5 a significantly higher brain AUC was observed for intranasal ATX-Muco Lipo (8.88 min %/g) and intranasal ATX+PHE-Muco Lipo (2.26 min %/g) when compared with intravenous ATX-Lipo (1.28 min %/g) indicating the efficiency of the liposomes for brain targeting.

The BBR of 0.161, 1.255, 0.331, 0.003 for ATX-Lipo (i. n.), ATX-Muco Lipo (i. n.) ATX+PHE-Muco Lipo (i. n.), ATX-Lipo (i. v.) respectively at 30 min indicate greater transport of drug to the brain after intranasal administration of liposomal formulations compared to intravenous administration of liposomes which is represented in fig.1. This could be indicative of direct transport of the liposomes bypassing the blood brain barrier due to a direct connection between the nose and brain because of the olfactory region present in the nasal cavity [28, 29].

The drug (ATX) targeting efficiency (DTE, %) and brain drug (ATX) direct transport percentage (DTP, %) were also calculated for nasally administered formulations from the pharmacokinetic data depicted in table 4. As shown in table 6 amongst the nasally administered formulations, ATX-Muco Lipo and ATX+PHE-Muco Lipo formulations showed greater DTE (%) and DTP (%) values followed by ATX-Lipo. Five-fold higher DTE (%) and three-fold higher DTE (%) for ATX-Muco Lipo and ATX+PHE-Muco Lipo respectively compared to ATX-Lipo demonstrated the significance of the mucoadhesive liposomal formulation. Similar studies have reported such results for nose-to-brain targeted intranasal mucoadhesive micro emulsion drug delivery systems [9, 30].

On application of Student's t-test, no statistically significant difference was found between intranasal and intravenous routes of administration. Hence, in the present study to obtain statistically significant results there was a need for extensive animal studies. However, within the limits of the experimental design above results were obtained.

**Table 6: Drug targeting efficiency and Direct transport percentage\* derived following intranasal administration of <sup>99m</sup>Tc-ATX Lipo (intranasal), <sup>99m</sup>Tc-ATX Muco Lipo (intranasal), <sup>99m</sup>Tc-ATX+PHE Lipo (intranasal), <sup>99m</sup>Tc-ATX+PHE Muco Lipo (intranasal) formulations**

Formulation and route of administration	DTE %	DTP %
ATX-Lipo i.n.	52.13±2.34	98.08±0.16
ATX Muco-Lipo i.n.	251.41±3.05	99.60±0.11
ATX+PHE-Muco Lipo i.n.	182.21±4.21	99.45±0.32

\* Parameters are derived using mean±SD.

In order to visualize brain uptake following intranasal administration of <sup>99m</sup>Tc tagged ATX solution and ATX-Lipo formulation gamma camera was used. The use of gamma ray emitting radionuclide <sup>99m</sup>Tc helped to perform imaging studies to complement the information obtained from tissue distribution experiments. fig. 4 and 5 depict the gamma scintigraphic images for intranasal ATX solution and intranasal ATX+PHE Muco Lipo respectively at 30 min post administration in rats. This was consistent with the results obtained from fig. 1 and table 5.

From fig. 4 and 5 it was observed that most of the radiolabeled intranasal drug solution and liposomal formulation appeared in the stomach of rat. Similar results were also reported by Patel *et al.* for intranasal brain targeted risperidone solid lipid nano particles [31]. This is also supported by the graphical depiction of the bio distribution of the radiolabeled drug in various organs of rat in fig. 6 and 7 after intranasal and intravenous administration of formulation respectively. However, a considerable amount of drug was seen in the brain for intranasal ATX+PHE Muco Lipo as compared to intranasal ATX solution at 30 min post administration.



**Fig. 4: ATX solution (intranasal)**



**Fig. 5: ATX+PHE muco lipo (intranasal)**

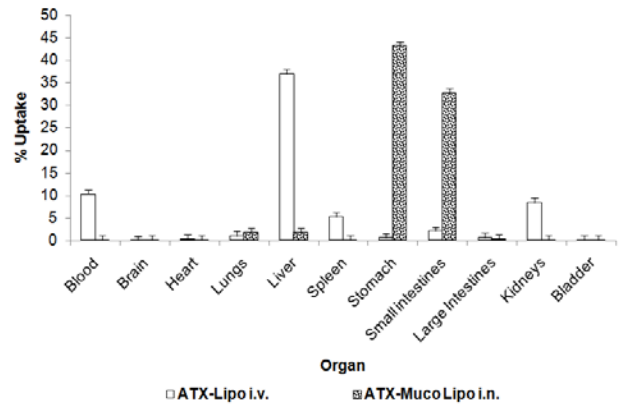


**Fig. 6: Bio distribution of (A) ATX-Lipo (intravenous) and (B) ATX-Muco Lipo (intranasal) after 30 min. The values represent mean±SD of three animals, p<0.05**

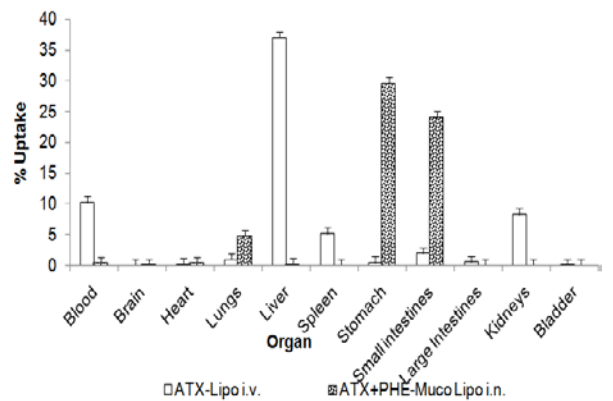


**Fig. 7: Biodistribution of (A) ATX-Lipo (intravenous) and (B) ATX+PHE-Muco Lipo (intranasal) after 30 min. The values represent mean±SD of three animals, p<0.05**

**CONCLUSION**

In the present investigation, the utility of liposomes as a carrier for nasal delivery of ATX was studied. All formulations were successfully formulated, characterized and found suitable for intranasal administration. The preliminary results of this investigation along with the *in vivo* studies demonstrated the potential delivery of ATX to brain via a nasal route from formulations containing mucoadhesive polymer HPMC and vasoconstrictor phenylephrine i.e. ATX-Muco Lipo and ATX+PHE-Muco Lipo. It also demonstrates the existence of nose-to-brain transport of ATX as evident through the gamma scintigraphy results.

However, further detailed animal experimentation with a greater number of animals being sacrificed at more time points is warranted in order to obtain statistically significant results.

**ACKNOWLEDGEMENT**

Authors are thankful to University Grants Commission, India for providing financial support for carrying out this investigation.

Authors are also thankful to Radiation Medicine Centre, Tata Memorial Hospital, Parel, Mumbai for providing all facilities and permitting us to carry out experimental work.

#### CONFLICT OF INTERESTS

Declared none

#### REFERENCES

1. Faraone SV, Sergeant J, Gillberg C, Biederman J. The worldwide prevalence of ADHD: is it an American condition? *World Psychiatry* 2003;2:104.
2. Madaan V, Kinnan S, Daughton J, Kratochvil CJ. Innovations and recent trends in the treatment of ADHD; 2006.
3. De Sousa A, Kalra G. Drug therapy of attention-deficit hyperactivity disorder: current trends. *Mens Sana Monograph* 2012;10:45.
4. Sauer JM, Ring BJ, Witcher JW. Clinical pharmacokinetics of atomoxetine. *Clin Pharmacokinet* 2005;44:571-90.
5. Löscher W, Potschka H. Blood-brain barrier active efflux transporters: ATP-binding cassette gene family. *NeuroRx* 2005;2:86-98.
6. Elshafeey AH, Bendas ER, Mohamed OH. The intranasal microemulsion of sildenafil citrate: *in vitro* evaluation and *in vivo* pharmacokinetic study in rabbits. *AAPS PharmSciTech* 2009;10:361-7.
7. Fazil M, Haque S, Kumar M, Baboota S, Sahni JK, Ali J. Development and evaluation of rivastigmine loaded chitosan nanoparticles for brain targeting. *Eur J Pharm Sci* 2012;47:6-15.
8. Mahajan HS, Mahajan MS, Nerkar PP, Agrawal A. Nanoemulsion-based intranasal drug delivery system of saquinavir mesylate for brain targeting. *Drug Delivery* 2014;2:148-54.
9. Vyas TK, Babbar A, Sharma R, Singh S, Misra A. Intranasal mucoadhesive microemulsions of clonazepam: preliminary studies on brain targeting. *J Pharm Sci* 2006;95:570-80.
10. Jogani VV, Shah PJ, Mishra P, Mishra AK, Misra AR. The intranasal mucoadhesive microemulsion of tacrine to improve brain targeting. *Alzheimer Dis Assoc Disord* 2008;22:116-24.
11. Haque S, Sahni JK, Ali J, Baboota S. Development and evaluation of brain targeted intranasal alginate nanoparticles for treatment of depression. *J Psychiatr Res* 2014;48:1-12.
12. Biju S, Talegaonkar S, Mishra P, Khar R. Vesicular systems: an overview. *Indian J Pharm Sci* 2006;68:141.
13. Arumugam K, Subramanian G, Mallayasamy S, Averineni R, Reddy M, Udupa N. A study of rivastigmine liposomes for delivery into the brain through intranasal route. *Acta Pharm* 2008;58:287-97.
14. Shinde LR, Jindal BA, Devarajan VP. Microemulsions and nanoemulsions for targeted drug delivery to the brain. *Curr Nanosci* 2011;7:119-33.
15. Dhuria SV, Hanson LR, Frey WH. Novel vasoconstrictor formulation to enhance intranasal targeting of neuropeptide therapeutics to the central nervous system. *J Pharmacol Exp Ther* 2009;328:312-20.
16. Hathout RM, Mansour S, Mortada ND, Guinedi AS. Liposomes as an ocular delivery system for acetazolamide: *in vitro* and *in vivo* studies. *AAPS PharmSciTech* 2007;8:1-12.
17. Aher ND, Nair HA. Bilayered films based on novel polymer derivative for improved ocular therapy of gatifloxacin. *Sci World J* 2014. Doi.org/10.1155/2014/297603. [Article in Press]
18. Saha GB. *Physics and Radiobiology of Nuclear Medicine*. Springer; 2010.
19. Kumar M, Misra A, Mishra A, Mishra P, Pathak K. Mucoadhesive nanoemulsion-based intranasal drug delivery system of olanzapine for brain targeting. *J Drug Targeting* 2008;16:806-14.
20. Glavas-Dodov M, Fredro-Kumbaradzi E, Goracinova K, Simonoska M, Calis S, Trajkovic-Jolevska S, et al. The effects of lyophilization on the stability of liposomes containing 5-FU. *Int J Pharm* 2005;291:79-86.
21. Caddeo C, Teskač K, Sinico C, Kristl J. Effect of resveratrol incorporated in liposomes on proliferation and UV-B protection of cells. *Int J Pharm* 2008;363:183-91.
22. Law S, Huang K, Chou V, Cherng J. Enhancement of nasal absorption of calcitonin loaded in liposomes. *J Liposome Res* 2001;11:165-74.
23. Laouini A, Jaafar-Maalej C, Sfar S, Charcosset C, Fessi H. Liposome preparation using a hollow fiber membrane contactor—Application to spironolactone encapsulation. *Int J Pharm* 2011;415:53-61.
24. Ugwoke MI, Sam E, Van Den Mooter G, Verbeke N, Kinget R. Nasal mucoadhesive delivery systems of the antiparkinsonian drug, apomorphine: influence of drug-loading on *in vitro* and *in vivo* release in rabbits. *Int J Pharm* 1999;181:125-38.
25. Charlton ST, Davis SS, Illum L. Evaluation of the effect of ephedrine on the transport of drugs from the nasal cavity to the systemic circulation and the central nervous system. *J Drug Targeting* 2007;15:370-7.
26. Järvinen K, Urtti A. Duration and long-term efficacy of phenylephrine-induced reduction in the systemic absorption of ophthalmic timolol in rabbits. *J Ocul Pharmacol Ther* 1992;8:91-8.
27. Kyyrönen K, Urtti A. Effects of epinephrine pretreatment and solution pH on the ocular and systemic absorption of ocularly applied timolol in rabbits. *J Pharm Sci* 1990;79:688-91.
28. Thakkar HP, Patel AA, Chauhan NP. The intranasal mucoadhesive microemulsion of mirtazapine: pharmacokinetic and pharmacodynamic studies. *Asian J Pharm* 2013;7:36.
29. Patel MR, Patel RB, Bhatt KK, Patel BG, Gaikwad RV. Paliperidone microemulsion for nose-to-brain targeted drug delivery system: a pharmacodynamic and pharmacokinetic evaluation. *Drug Delivery* 2016;23:346-54.
30. Vyas TK, Babbar A, Sharma R, Misra A. Intranasal mucoadhesive microemulsions of zolmitriptan: preliminary studies on brain-targeting. *J Drug Targeting* 2005;13:317-24.
31. Patel S, Chauhan S, Soni H, Babbar A, Mathur R, Mishra A, et al. Brain targeting of risperidone-loaded solid lipid nanoparticles by the intranasal route. *J Drug Targeting* 2011;19:468-74.